Contrib Mineral Petrol (2003) 145: 612–627
DOI 10.1007/s00410-003-0474-x

ORIGINAL PAPER

H. M. Rajesh

Outcrop-scale silicate liquid immiscibility from an alkali syenite (A-type granitoid)-pyroxenite association near Puttetti, Trivandrum Block, South India

Received: 11 October 2002 / Accepted: 23 March 2003 / Published online: 21 June 2003

Abstract The Pan-African (572 Ma) Puttetti syenite (A-type granitoid)-pyroxenite association intrudes the high-grade metamorphic terrain of the Trivandrum Block, South India. Field evidence indicates the contemporaneous nature of syenitic and pyroxenitic liquids. The occurrence of a mixed-rock (~70% syenite and 30% pyroxenite) with an emulsion-like texture, and the occurrence of pyroxenite globules in syenite, is interpreted as relics of immiscible magmas. Both syenite and pyroxenite show similar mineral assemblage (with major minerals having overlapping compositions), but the relative proportions differ. Major element and trace element partitioning trends, parallel REE patterns, and similar Sr initial isotope compositions are in accord with behavior either predicted or measured for immiscible melts in experimental and/or natural systems. The more pronounced Eu anomalies and LREE/HREE ratios of syenite and pyroxenite (relative to the mixed-rock) is related to fractionation caused by immiscible separation. The proposed origin of the Puttetti pluton involves the intrusion of a magma whose bulk composition is that of the mixed-rock. This melt behaved immiscibly and split into two fractions, which produced the syenite and pyroxenite magmas.

Introduction

Silicate liquid immiscibility has often been called upon to explain the juxtaposition of mafic (Fe-rich basic) and silicic (K-rich silicic) rocks in a variety of igneous suites (see references given by Roedder 1979), and as a petrogenetic process has provoked much discussion in the literature. Although most of the published works address immiscibility at a microscopic scale (where the two immiscible liquids exist as discrete glasses), a few studies have addressed the possible criteria to illustrate liquid immiscibility at a larger scale (e.g. Bender et al. 1982; Ferreira et al. 1994). If immiscibility is to produce sizable bodies of contrasting magmas, it appears necessary for magma to first fractionally crystallize, so that when unmixing does take place, the conjugate liquids are free to separate (Philpotts 1982). Simple liquid-liquid blending is likely to occur in systems where the end-members do not differ greatly in temperature, and where there is an appropriate proportion of mafic end member. This study evaluates liquid immiscibility at the outcrop scale near Puttetti, Trivandrum Block, South India, using all pertinent field, petrographic, chemical, and isotopic data. Evidence is presented to show that liquid immiscibility occurred prior to the emplacement of mixed-rock magma of intermediate composition to produce alkali syenite (A-type granitoid) and associated pyroxenite of the Puttetti pluton. It is suggested that the mixed-rock resulted from crystal fractionation in a deep-seated chamber of alkali basalt magma followed by liquid-liquid unmixing. This is one of the clearest examples of mutual exsolution of two natural silicate liquids having compositions, of syenite and pyroxenite, similar to the general compositional nature of conjugate liquids in alkaline rocks suggested by Philpotts (1982).

H. M. Rajesh
Gondwana Institute for Geology and Environment,
147–2 Hashiramoto, 648-0091, Hashimoto, Japan
E-mail: rajeshuu@yahoo.com

Present address: H. M. Rajesh
Department of Geosciences, The University of Queensland,
Steele Bldg., St Lucia 4072, Australia

Editorial responsibility: T. Grove

Geologic setting

The high grade terrain of the Trivandrum Block forms a significant portion of the South Indian shield area, and consists of the Achankovil metasedimentary rocks (within the Achankovil Shear Zone; ASZ), the Kerala Khondalite Belt (KKB) and the Nagercoil charnockite massif (Fig. 1). To the northeast of this block, and

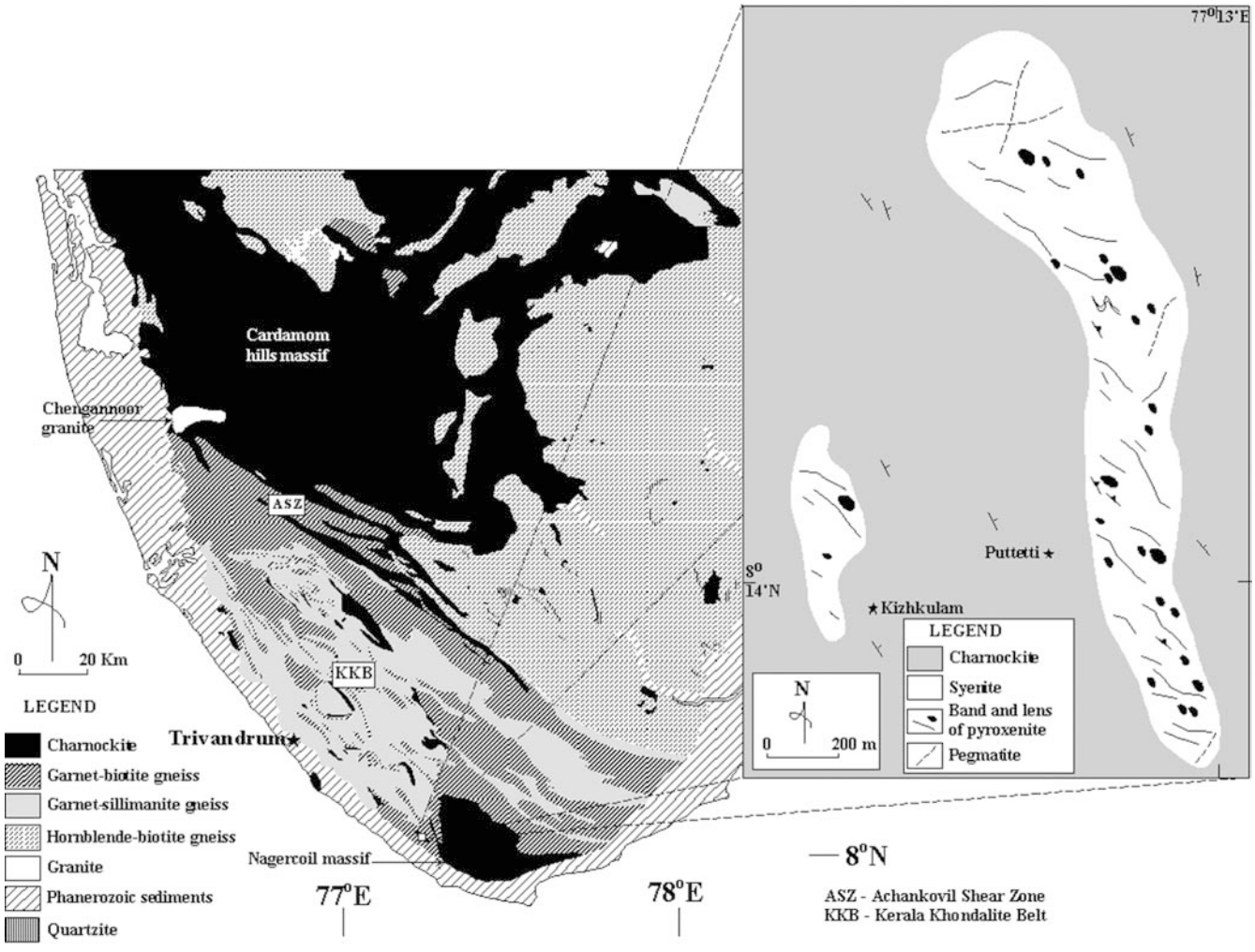

Fig. 1 Generalized geologic map of southern India showing the major units and the present study area. The enlarged box shows the geologic map of Puttetti and its adjoining areas. The approximate distribution pattern of pyroxenite lenses and bands in the syenite is shown and is not to scale

separated by the ASZ, is the homogeneous, garnet- and graphite-free Cardamom Hills charnockite massif. The Trivandrum Block exposes a varied assemblage of orthopyroxene, hornblende, and biotite (± garnet)-bearing intermediate to acid granulites of broadly granitic composition (charnockites to charnoenderbites), basic granulites, garnet-biotite-sillimanite ± cordierite-bearing paragneisses (khondalites), garnet-biotite gneisses (leptynitic paragneisses and granitic augen gneisses), calc-silicate gneisses, cordierite gneisses, and a host of acid and basic intrusions (Fig. 1). Recent studies have suggested a metamorphic history with a period of isobaric cooling (e.g. Satishkumar and Harley 1998) followed by a period of decompression for the Trivandrum Block (e.g. Nandakumar and Harley 2000), indicating multiple stages of metamorphism. The earliest recorded (poorly defined) metamorphism was identified as ca. 1.8–2.0 Ga, overprinted by the granulite facies metamorphism at ca. 600–540 Ma at conditions of 4.2–9.5 kb, 750–1,000 °C and under high geothermal gradients (40–150°/km) (see Nandakumar and Harley 2000 and references therein).

Three alkali granites (along the ASZ) and one syenite pluton (Puttetti syenite (this study) near the Nagercoil massif) have been reported from the Trivandrum Block. Available geochronologic data indicate that these intrusives preserve evidence for the Pan-African felsic magmatic event (~550–640 Ma; Rajesh 1999 and references therein) recognized in south-western India by Rajesh et al. (1996). These intrusives are considered to represent anorogenic or post-orogenic A-type magmas generated in rift-related environments of high heat flow and abundant volatile activity, correlative with a post-collisional (collision being that of fragments of East and West Gondwana) extensional tectonic regime and probably including melts generated from both upper mantle and lower crustal sources. The concentration of Pan-African granitic magmatism in a broad region of granulite facies metamorphism in East Gondwana points to a high temperature event either above a rising plume or a zone of rifting (Rajesh 1999).

Study area and field relations

This study concentrates on the Puttetti syenite-pyroxenite association, near the Nagercoil massif, and is within the Trivandrum Block. The Puttetti syenite-pyroxenite association is exposed as a NNW–SSE elongated pluton geomorphically expressed as a continuous low ridge near the Puttetti area (Fig. 1). The intrusive is spatially related to the intersection point of a NW–SE trending fault lineament with a NE–SW trending seismically active deep fault (Grady 1971). The syenite was studied by Nair and Santosh (1985) and is noted for its large crystals of zircon, leading to some interesting scientific investigations (e.g. Murali et al. 1983; Santosh 1985).

The geologic literature contains descriptions of localities where the field relations reveal apparent immiscibility textures (e.g. Bender et al. 1982; Ferreira et al. 1994). The evidence bearing upon liquid-liquid phase separation is described here together with the field relations of the Puttetti pluton. Puttetti syenite is a massive medium- to coarse-grained, greenish-grey to grey rock composed dominantly of feldspar and pyroxene with minor amphibole and biotite. Magmatic-state fabric is characterized by linear, sometimes planar orientations of feldspar and mafic grains. Lenses and bands of pyroxenite varying in thickness from 0.1–0.5 cm are found within the syenite (Fig. 2a), and occur in swarms, commonly parallel to the flow foliation of the host syenite. The mineral assemblage of the pyroxenite inclusions is the same as that of the host syenite, but the proportions of the minerals differ. These inclusions are uniformily distributed and are variable in size. They have about the same grain size as the host syenite. The contact is physically sharp, suggesting that the two magmas were not miscible. At places, alternating mafic and felsic bands give rise to a banded appearance, sometimes persisting for many meters along strike. Locally the inclusions are plastically folded (Fig. 2b), which indicates that both pyroxenite and syenite responded plastically during intrusion. The syenite is cut by a few late stage, syenitic and pyroxenitic dykes, and composite dykes having pyroxenitic margins and coarse-grained syenitic cores. The core of one of the pyroxenitic dykes is significantly calcite-rich (Fig. 2c), indicating the extent of fluid activity in the pluton. The presence of pyroxenite also as syn-plutonic and late-stage dikes argues for the contemporaneous nature of the two liquids. Obvious features that can be related to mingling and incomplete mixing of two independent, contemporaneous magmas (mixing zones, chilled margins, double enclaves, zoned enclaves; Vogel and Wilband 1978; Vernon 1983) are absent in the pluton.

At places, inclusions of a mixed-rock (about 70% syenite and 30% pyroxenite), although limited, are seen within the pluton (Figs. 2d, e). This rock shows a fine-medium grain size and has an emulsion-like texture with a mixture of one liquid in the other. Near its contact with the pyroxenite, the syenite contains numerous pyroxenite globules ranging in size from less than 1 mm to several centimeters (Fig. 2f). This is similar to some tholeiitic basalts where globules of iron-rich liquid typically form in the silica rich host (e.g. Philpotts 1978), and may reasonably be interpreted as relics of immiscible magmas with the unmixing of the mixed-rock liquid initiated by the separation of rounded globules of the pyroxenitic phase in a syenitic matrix. The shape of the globules varies with smaller globular structures being spherical or sub spherical to larger ones being ellipsoidal (often elongated along a preferential direction) to irregular (with inward pointing cusps around their margins, the points of the cusps pointing towards the quartzofeldspathic liquid), consistent with the corollary that the larger the globule, the more easily it is deformed (Roedder 1979). Deformation of globules would certainly be expected if the physical separation of immiscible liquids had taken place at depth. Sometimes adjacent globules impinge and coalesce with one another (Figs. 2h, i). The contact of two coalescing globules is characterized by amoeboid boundaries; the interfacial tension between liquids possibly not permitting the persistence of sharp curved boundaries (Philpotts 1978). The syenite commonly coexists with a pegmatite facies and, significantly, small globules of pyroxenite are seen near their contact with the syenite (Fig. 2i). Phase separation seems to have occurred prior to intrusion as flow differentiation commonly appears to have affected the distribution of the globules.

An important feature of the Puttetti pluton is its mineral wealth, including zircon, phlogopite, molybdenite, chevkinite and magnetite. The coarse grained portions of the syenite carry brown or honey yellow coloured, large, euhedral crystals of zircon measuring up to 5 cm, the most common variety showing an elongation along the c-axis. This is unique to Puttetti syenite, which distinguishes it from other quartz-alkali feldspar syenites of south-western India. Phlogopite concentration is seen in the syenite near the contact with the pyroxenite as well as within the pyroxenite. In addition to its presence as an accessory phase in the syenite, phlogopite also tends to concentrate in the mafic-rich portions of the syenite. Disseminated molybdenite is seen within the syenite. Reddish black elongated chevkinite crystals (sometimes $\sim$0.1 m in length in the elongated direction) occur in the associated pegmatites. These alkaline pegmatites also contain large crystals of magnetite. Magnetite is usually associated with quartz, while chevkinite is usually associated with alkali feldspar.

Wherever the contact is discernible (the contact is often obscure due to profound laterization), the syenite shows an intrusive relationship with the surrounding qtz-kfs-opx-grt-bt bearing dark greenish-grey massive charnockite. No chilled margin was observed. Gneissic structure is weakly developed with a general NW–SE foliation. An acid variant with smaller amounts of ferromagnesian minerals occurs towards the western part of the study area. The gneissic rocks in the study area show variations from a predominant garnet-biotite

gneissic rock, through an intercalated rock of garnet-biotite gneiss and garnet leuco-gneiss, to bands of augen gneiss. Irregular patches ($\sim$ 0.5–20 cm) and veins of charnockite (arrested charnockite) are spectacularly exposed in the garnet-biotite gneiss. Pegmatites (containing graphite), occurring as meter-scale segregations and veins, often cut across the gneisses. At one exposure granitic veins (graphite absent; probably later than pegmatites) cut both the arrested charnockite and the host garnet-biotite gneiss. These veins are surrounded by hydration haloes resulting in the conversion of portions, of arrested charnockite as well as its host garnet biotite gneiss, adjacent to the vein (within about 10 cm) to gneissose granite. Thus in the Puttetti area, field relations show a history of intrusion, dehydration, and hydration; the latest event being the retrogression of arrested charnockite.

Petrography and mineral chemistry

Modal, chemical (Fig. 3) and whole-rock XRD analyses (Rajesh 1999) indicate that the dominant rock type of the Puttetti pluton is a syenite. Quantitative analyses of the mineral phases was performed using an electron microprobe analyzer (Shimadzu EPMA-8705) utilizing the correction procedures of Bence and Albee (1968), or a SEM Jeol JED-2000 with the AUTOZAP program system and standardless ZAF correction. An operating voltage of 15 kV was maintained with a beam current of 1.5 nA. The syenite shows a medium- to coarse-grained hypidiomorphic granular texture and is dominated by phenocrysts of perthitic K-feldspar ($\sim$82%). Major minerals in the paragenesis are, in approximately decreasing order of abundance: K-feldspar (within a few mole percent of $An_4Or_{38}Ab_{58}$), clinopyroxene (hedenbergite or augite), plagioclase ($Ab_{90}An_{10}$—$Ab_{85}An_{15}$), amphibole (edenitic hornblende), phlogopite and biotite (Rajesh 1999). Accessory phases include zircon, Fe-Ti oxides (magnetite with subordinate ilmenite), apatite, titanite, corundum, quartz, epidote, calcite, chlorite and sulfide phases (pyrite/chalcopyrite). Calcite occurs as a late intercumulus phase at the interfaces of K-feldspar grains or as veins cutting across them.

Pyroxenites show a medium-grained phaneritic texture, with the main paragenesis consisting of hedenbergite or augite (dominant), perthitic K-feldspar, amphibole (hastingsitic hornblende to edenitic hornblende), phlogopite, and biotite (Rajesh 1999). Accessory phases include apatite, titanite, garnet, zircon, Fe-Ti oxides (magnetite with subordinate ilmenite) and sulphide phases (pyrite/chalcopyrite).

Bowen (1928) noted that immiscible liquids, which are in equilibrium, must crystallize phases in equilibrium, that is, rocks related through silicate liquid immiscibility should have similar mineral assemblages (with overlapping chemical compositions). However, because of the differences in liquid compositions, the proportions of minerals formed in each phase on cooling will be quite different. Mineral components of pyroxenite are similar to those in syenite, but the relative proportions differ. Clinopyroxenes from the Puttetti rocks (Rajesh 1999) have overlapping compositions (Fig. 4a; Table 1), consistent with an origin as immiscible liquid fractions. The amphiboles from the Puttetti rocks show a restricted range in composition from hastingsitic hornblende to edenitic hornblende (Fig. 4b; Table 1; Rajesh 1999). Further, their phlogopite compositions are also comparable (Fig. 4c; Table 1). Other petrogenetic processes (particularly crystal fractionation or incomplete magma mixing) are unlikely to produce magmas of differing bulk compositions (see next section) with minerals of overlapping composition. Further, the absence of any disequilibrium texture (e.g. sieved, dusty or fritted texture, rounded and embayed crystals, lath trails in K-feldspars, polyphase morphologies of apatite and plagioclase, reaction rims on hydrous phases, and pseudomorphs after mafic phases; Kuşcu and Floyd 2001 and references therein), the absence of heterogenous core-rim compositions, and normally and reversely zoned crystals in the same sample (e.g. Hibbard 1981; Halsor and Rose 1991), and the absence of textures indicating chemical diffusion between coexisting mafic and felsic magmas (e.g. hydration; Wiebe 1993) in Puttetti rock samples argue against a model involving mingling and incomplete mixing of two contemporaneous magmas.

Whole-rock element variations

Nair and Santosh (1985) presented major and trace element trends of the Puttetti syenite and pyroxenite. In addition to their data, a new set of major, trace and REE data from the Puttetti syenite, pyroxenite and mixed-rock is presented here (Table 2). Major and trace element contents of the Puttetti samples were determined by a Rigaku RIX-2000 X-ray fluorescence spectrometer on glass beads. Volatiles were determined by loss on ignition. Representative Puttetti samples were analysed for REEs by ICP-MS (Plasma Quad PQ1) on trace element solutions after separation of major elements through ion-exchange resins. The operating parameters and analytical precision are illustrated in Balaram et al. (1996) and the references therein.

The syenite has high K_2O (up to 6 wt%), and is metaluminous similar to quartz syenites worldwide and different from alkali-feldspar syenites which are mostly peralkaline. Features like high total alkalis ($Na + K \sim 11$ wt%), high Fe/Mg, low CaO and MgO, medium TiO_2/MgO of the Puttetti syenite are typical of A-type granitoids (e.g. Collins et al. 1982), similar to other quartz syenites from southwestern India (e.g. Fig. 5a; Rajesh 1999) and Pan-African post-collisional syenites from Madagascar and East Antarctica (see Fig. 5). According to Frost et al. (2001) geochemical classification for granitoid rocks, Puttetti syenite

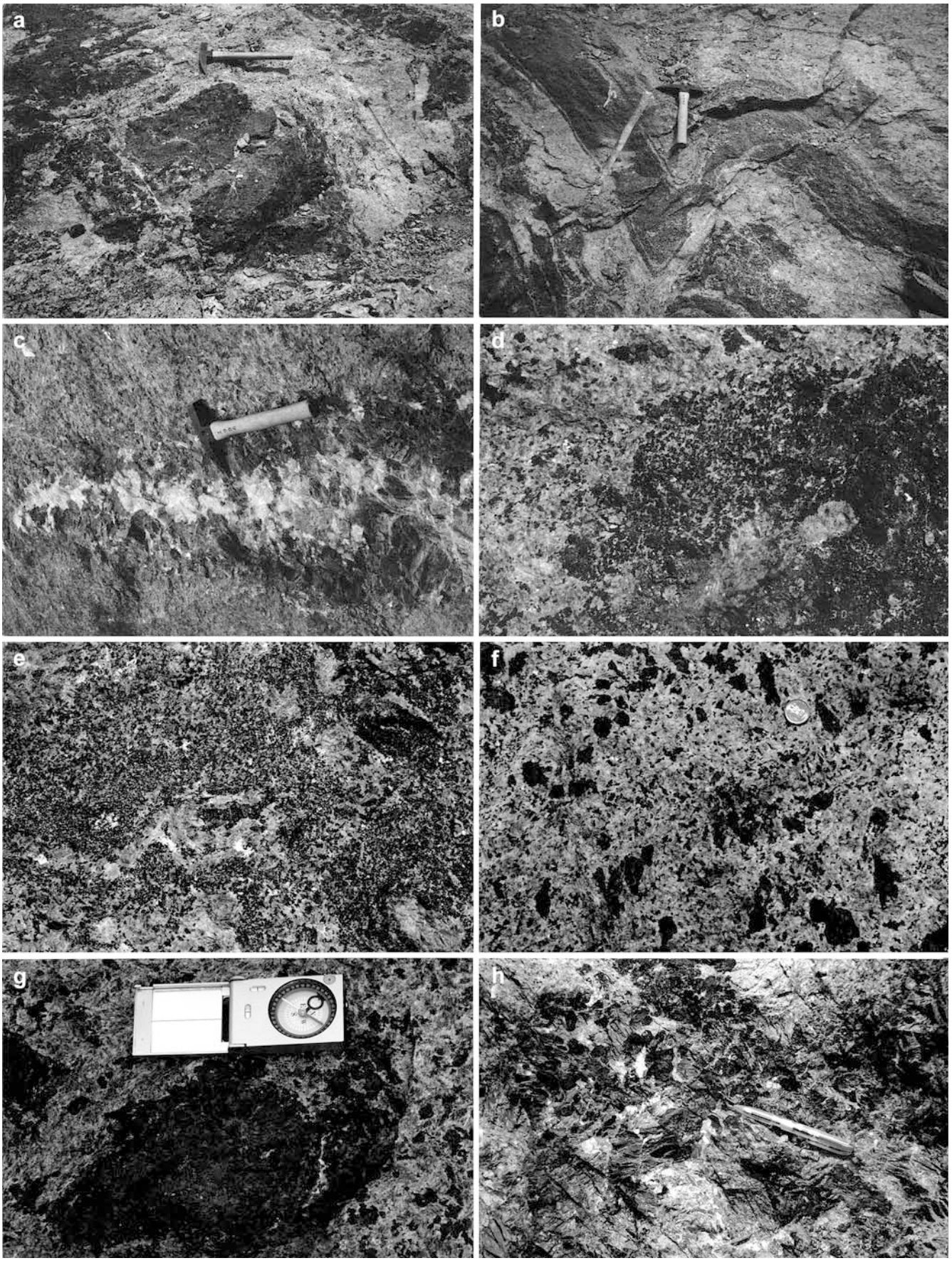
a
b
c
d
e
f
g
h

◀

Fig. 2a–h Field occurrence of syenite and pyroxenite at Puttetti. **a** Pyroxenite lens in syenite, with sharp contact and smooth outline. **b** Folded pyroxenite band in syenite, indicating that both syenite and pyroxenite responded plastically during intrusion. **c** Pyroxenitic dyke with calcite-rich core, indicating the extent of fluid activity in the pluton. **d** Mixed-rock inclusion in syenite. **e** Mixed-rock inclusion in syenite. Length of the pen is approx. 15 cm. **f** Pyroxenite globules in syenite. Some of these globules impinge and coalesce with one another. Diameter of the coin is approx. 2 cm. **g** Pyroxenite globules in syenite near a pyroxenite lens. **h** Pyroxenite globules (upper half of the photograph) in syenite near a pegmatite

samples are ferroan (in terms of Fe-number), alkalic (in terms of the modified alkali-lime index (MALI)), and metaluminous [in terms of aluminum saturation index (ASI)], appropriate to be classified as A-type granitoids (e.g. Fig. 5b).

Major element trends in Fig. 6 show that the syenite and pyroxenite samples lie on either end of a differentiation trend with mixed-rock samples occupying an intermediate position, towards the syenite end (the trend is more apparent in the case of trace elements). This indicates possible evolution of syenite and pyroxenite from the mixed-rock. When the major element concentrations of syenite and pyroxenite are normalized to the corresponding concentrations in the mixed-rock, it follows that the essential difference in chemical compositions of the syenite and pyroxenite is the preferential partitioning of all elements except SiO_2, Al_2O_3, Na_2O and K_2O into the latter (Fig. 7). This kind of major

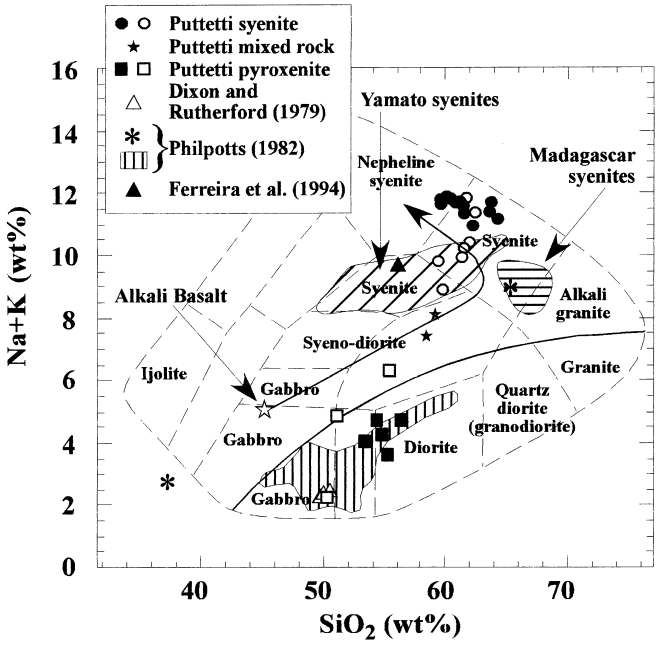

Fig. 3 Total alkali vs. silica diagram showing the chemical classification and nomenclature of Puttetti syenite, pyroxenite and mixed-rock samples. Regarding Puttetti samples, *open symbols* are data from Nair and Santosh (1985) and *closed symbols* are from this study. The thick line separates alkaline rocks from tholeiitic ones. Possible fractionation trend of alkali basalt (open star) is from Cox et al. (1979). The compositional range of tholeiitic basalts with immiscible glasses (*vertically ruled area*) and average composition of immiscible liquids preserved as glassy globules (Fe-rich glass and Si-rich glass) in alkaline basalts from Philpotts (1982) are given. Tholeiitic basalts showing immiscibility from Dixon and Rutherford (1979) and mixed-rock sample from Ferreira et al. (1994) are also shown. Pan-African post-collisional syenites from Madagascar and Yamato mountains, East Antarctica, are from Nédélec et al. (1995) and Zhao et al. (1995) respectively

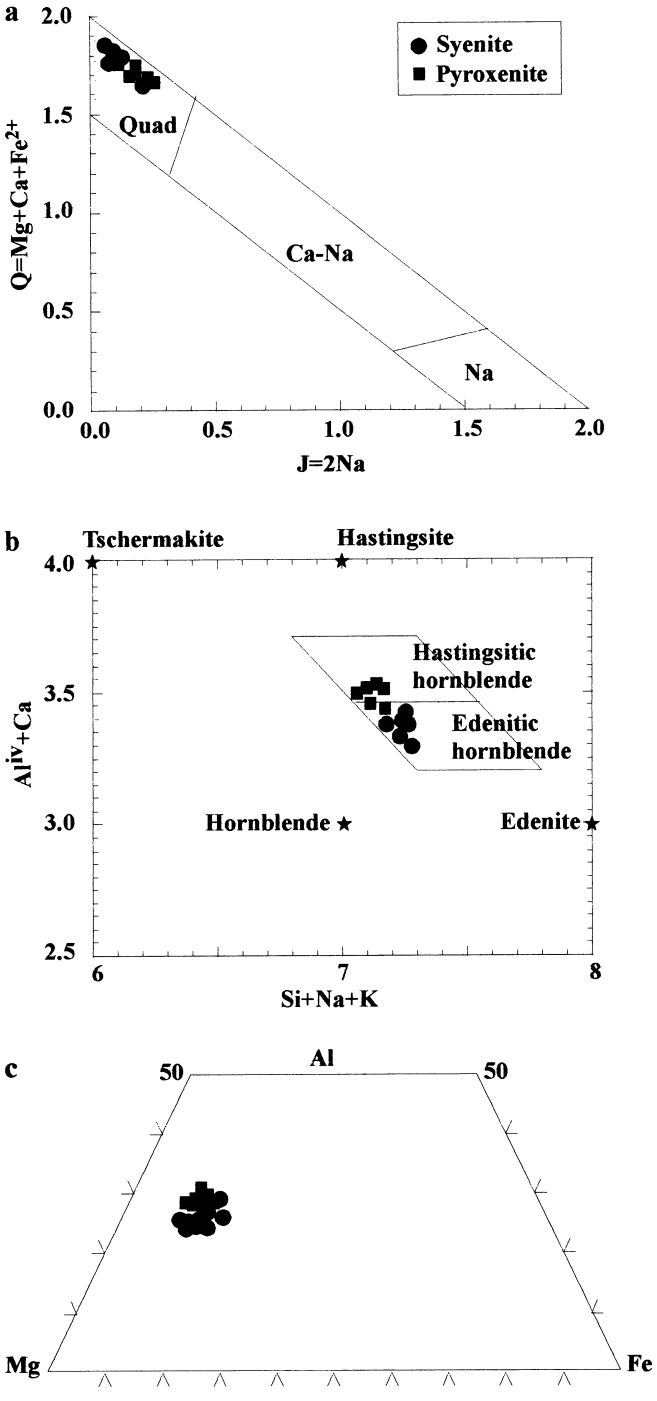

Fig. 4a–c Chemical composition of mafic minerals from Puttetti syenite and pyroxenite. **a** Pyroxene. **b** Amphibole. *Stars* indicate end member compositions. **c** Phlogopite

Table 1 Representative chemical composition of pyroxene, amphibole, and phlogopite from the Puttetti syenite and pyroxenite samples

	R96PU2s[a] Pyroxene	R96PU2p[a] Pyroxene	R98PU18s[a] Pyroxene	R98PU18p[a] Pyroxene	R96PU14s[a] Pyroxene	R96PU14p[a] Pyroxene	R98PU10s[a] Amphibole	R98PU10p[a] Amphibole	R96PU21s[a] Amphibole	R96PU21p[a] Amphibole	R98PU4s[a] Phlogopite	R98PU4p[a] Phlogopite
SiO_2	46.83	47.22	48.20	46.38	46.71	47.38	44.02	42.10	43.51	42.23	40.35	40.04
TiO_2	0.38	0.39	0.27	0.24	0.42	0.24	1.90	2.20	1.73	1.05	2.39	2.51
Al_2O_3	0.99	1.06	1.11	0.78	0.99	0.93	9.80	10.74	8.58	9.03	13.50	11.96
FeO[b]	28.37	29.17	26.56	28.56	27.21	27.32	12.44	14.30	19.13	20.13	7.41	7.85
MnO	0.61	0.40	0.60	0.56	0.80	0.74	0.10	0.20	0.48	0.33	0.12	0.13
MgO	1.98	2.01	1.85	1.02	1.88	2.02	15.26	13.20	11.21	10.30	22.10	23.14
CaO	19.21	17.98	19.94	20.11	20.02	19.33	11.60	11.10	11.37	11.06	0.01	0.01
Na_2O	0.48	0.51	1.21	1.30	0.88	0.57	1.81	2.23	1.28	1.73	0.78	0.68
K_2O	0.01	0.08	0.00	0.02	0.03	0.06	0.82	0.54	1.08	0.94	9.69	9.58
Total	98.86	98.82	99.74	98.97	98.94	98.59	97.75	96.61	98.37	96.80	96.35	95.90
Oxygens	6	6	6	6	6	6	23	23	23	23	11	11
Si	1.931	1.950	1.949	1.904	1.914	1.953	6.483	6.341	6.583	6.536	2.876	2.880
Ti	0.012	0.012	0.008	0.007	0.013	0.007	0.210	0.249	0.197	0.122	0.128	0.136
Al	0.048	0.052	0.053	0.038	0.048	0.045	1.688	1.897	1.513	1.629	1.134	1.014
Al^{iv}	0.048	0.050	0.051	0.038	0.048	0.045	1.568	1.692	1.487	1.534		
Al^{vi}	0.000	0.002	0.002	0.000	0.000	0.000	0.120	0.205	0.026	0.095		
Fe	0.979	1.008	0.899	0.981	0.932	0.942	1.520	1.792	2.394	2.577	0.442	0.472
Fe^{3+}	0.105	0.069	0.127	0.245	0.170	0.083	0.365	0.240	0.494	0.501		
Fe^{2+}	0.874	0.939	0.772	0.736	0.762	0.859	1.155	1.552	1.900	2.076		
Mn	0.021	0.014	0.021	0.019	0.028	0.026	0.012	0.026	0.062	0.043	0.007	0.008
Mg	0.122	0.124	0.112	0.062	0.115	0.124	3.351	2.964	2.529	2.377	2.348	2.481
Ca	0.849	0.796	0.864	0.884	0.879	0.854	1.830	1.791	1.843	1.834	0.001	0.001
Na	0.038	0.041	0.095	0.103	0.070	0.046	0.517	0.651	0.375	0.519	0.108	0.095
K	0.001	0.004	0.000	0.001	0.002	0.003	0.154	0.104	0.208	0.186	0.881	0.879
X_{Mg}	0.111	0.109	0.111	0.059	0.110	0.116	0.688	0.623	0.514	0.480	0.842	0.840
Wo	43.54	41.29	46.08	45.87	45.64	44.48						
En	6.26	6.42	5.97	3.22	5.97	6.46						
Fs	50.21	52.29	47.95	50.91	48.39	49.06						

[a]Average of 3–5 analyses
[b]Total iron as FeO; Fe^{3+} calculated by stochiometry; s, syenite; p, pyroxenite

Table 2 Representative major and trace element analyses of the Puttetti syenite, pyroxenite and mixed-rock samples. Major oxides, weight percent; trace elements, parts per million

Rock type	Syenite	Syenite	Syenite	Pyroxenite	Pyroxenite	Pyroxenite	Mixed rock
Major elements (wt%)	R95099122	R9509913	R96099162	R9509911	R9509916	R96099110	R96099183
SiO_2	60.11	59.17	62.02	56.02	53.98	52.96	59.05
TiO_2	0.43	0.39	0.18	0.98	1.02	1.10	0.34
Al_2O_3	18.02	16.76	17.35	7.11	6.58	7.12	12.15
Fe_2O_3[a]	6.26	7.62	5.03	10.51	10.90	11.30	5.63
MnO	0.12	0.12	0.05	0.22	0.39	0.22	0.07
MgO	0.33	0.28	0.98	7.41	4.81	5.42	5.44
CaO	1.57	1.66	2.20	12.95	14.59	15.22	8.18
Na_2O	5.71	5.86	5.42	2.87	2.59	2.21	4.52
K_2O	6.11	5.79	5.55	1.87	2.13	1.88	3.54
P_2O_5	0.06	0.07	0.09	0.46	1.02	0.33	0.46
LOI	0.83	0.90	0.81	0.82	1.41	0.86	0.68
Total	99.55	98.62	99.68	101.22	99.42	98.62	100.06
Na_2O/K_2O	0.93	1.01	0.98	1.53	1.22	1.18	1.28
R1	380	306	778	1,986	1,878	1,991	1,350
R2	538	520	624	1,893	1,929	2,037	1,383
ASI[b]	0.96	0.89	0.92	0.24	0.20	0.21	0.47
MALI[c]	10.25	9.99	8.77	−8.21	−9.87	−11.13	−0.12
Fe number[d]	0.95	0.96	0.84	0.59	0.69	0.68	0.51
Trace elements (ppm)							
Cr	12		12	4		7	
Ni	3	1	16	9	9	10	10
Rb	125	123	221	85	71	81	153
Sr	24	25	102	247	181	254	124
V	21	35	18	23	10	18	11
Y	19	19	22	124	251	138	100
Zn	201	159	71	420		390	225
Zr	771	557	450	482	455	411	187
Ba	70	41	602	657	213	642	577
Nb	48	49	45	19	24	21	40
Mo	3	2	6	3	1	3	5
Pb	5	5	2	0	0	0	1
Th	8	3	6	971	165	114	6
U	3	1	2	99	18	18	1
Tb	0	1	1	24	12	4	2
Ta	2	1	1	14	6	5	4
Hf	4	1	4	17	6	1	4
La	28	52	9	174	249	340	50
Ce	71	122	23	417	682	903	102
Pr	7	11	2	37	68	90	14
Nd	21	31	7	91	176	237	59
Sm	7	10	3	20	40	55	12
Eu	1	1	0	5	8	10	2
Gd	9	13	3	31	53	78	8
Tb	1	2	1	4	9	12	2
Dy	7	11	2	21	39	64	7
Ho	2	3	0	5	9	15	1
Er	3	5	0	8	15	26	4
Yb	6	9	1	11	21	42	6
Lu	1	1	0	3	3	6	1
Rb/Sr	5.15	4.85	2.17	0.35	0.39	0.32	1.24
K/Ba	721	1162	76	24	83	24	51
K/Rb	405	391	208	182	247	191	192

[a]Total Fe as Fe_2O_3
[b]Molar $Al_2O_3/(CaO + Na_2O + K_2O)$
[c]$Na_2O + K_2O - CaO$
[d]$Fe_2O_3^*/(Fe_2O_3^* + MgO)$

element partitioning is in accord with a silicate liquid immiscibility model of origin. Pyroxenite has a high Na_2O/K_2O ratio than syenite (see Table 2), consistent with experimental data (Naslund 1983) which demonstrated that the more iron-rich of the two coexisting immiscible liquids should have a higher Na_2O/K_2O ratio.

It has been suggested that one of the best way to explore the role of liquid immiscibility in the evolution of an igneous suite is with a pseudo-ternary diagram of the system silica-fayalite-leucite (Roedder 1979). In the (total $Fe + MnO + MgO + TiO_2 + CaO + P_2O_5$)–($Na_2O + K_2O + Al_2O_3$)–$SiO_2$ diagram (Fig. 8a) analyses of syenite and pyroxenite, which have a rather restricted compositional range, do not plot entirely within the low-temperature immiscibility field shown by Roedder (1951). Compositions of pyroxenite fall within the immiscibility field, but compositions of syenite plot outside that, at slightly

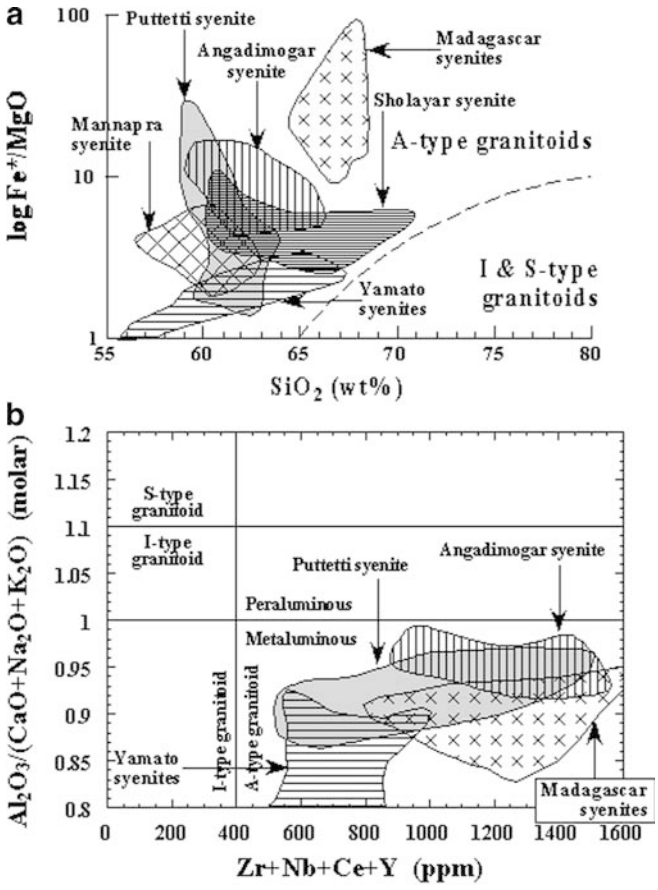

Fig. 5a, b Puttetti syenite samples plotted on discrimination diagrams of A-type, I-type and S-type granitoids. Data from other quartz syenites from south-western India (Rajesh 1999 and references therein) and Pan-African post-collisional syenites from Madagascar and Yamato mountains, East Antarctica are shown for comparison. **a** log Fe*/MgO vs. silica plot. Fe* is total Fe. **b** $Al_2O_3/(CaO + Na_2O + K_2O)$ (ASI) vs. Zr + Nb + Ce + Y plot

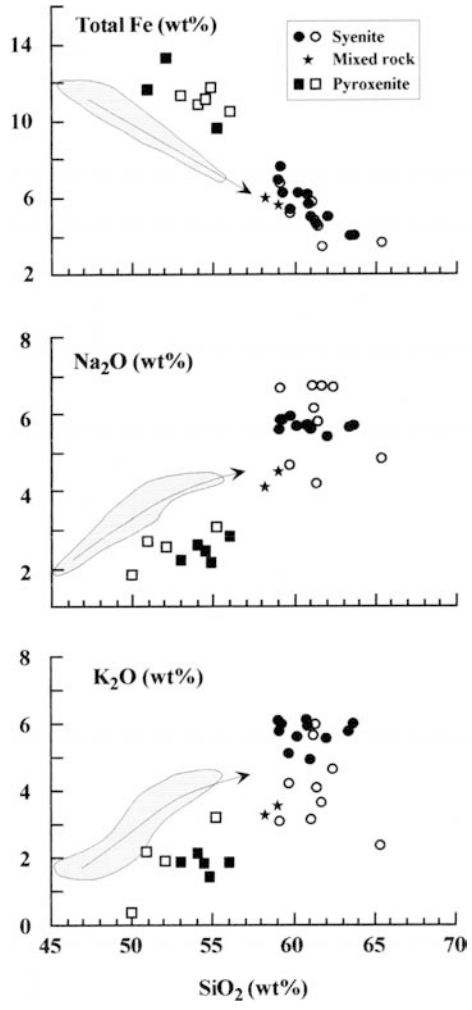

Fig. 6 Representative major element variation diagrams of the Puttetti syenite, pyroxenite and mixed-rock samples. *Open symbols* are data from Nair and Santosh (1985) and *closed symbols* are from this study. Data from Gough Island basalts (*shaded area*) and the corresponding trends (*dotted line*) of crystal fractionation of these basaltic magmas to generate intermediate rocks is also shown (Le Roex 1985)

higher concentrations of alkalis + alumina, as expected for alkaline rocks (Philpotts 1982). Freestone (1978) demonstrated that the addition of TiO_2 and P_2O_5 in the silica-fayalite-leucite pseudo-ternary system causes the two-liquid field (of Roedder 1951) to expand towards the leucite apex. In Fig. 8a Puttetti syenite samples lie on the two-liquid solvus of Freestone (1978). A similar compositional gap is also evidenced in the total Fe–$(Na_2O + K_2O)$–MgO diagram (Fig. 8b), where the analyses of syenite and pyroxenite fall near the edge of the immiscibility field shown by Philpotts (1976), with the syenite (A-type granitoid) compositions plotting towards the alkali corner.

Ti and P are minor elements which have often been utilized in the context of immiscibility since their partitioning during unmixing of magmas (felsic liquids are depleted in Ti and P relative to the basic liquids) deviates from that during normal fractional crystallization of basic magmas. On a ternary plot of P_2O_5, K_2O and TiO_2 (not shown), Puttetti samples show an overall linear trend from the K_2O apex to $\sim TiO_{2(70)}$ $P_2O_{5(30)}$ with the mixed rock samples between syenite and pyroxenite samples. Here the directional sense of the syenite and pyroxenite trends is away from the mixed rock. This trend cannot be due to fractional crystallization and can be best explained by liquid immiscibility, K_2O being strongly fractionated into the Si-rich liquid and TiO_2 and P_2O_5 into the Fe-rich liquid.

Further, in Fig. 9, syenite-pyroxenite pairs from Puttetti plot close to the field of analyses of natural and experimental glasses with undeniable origin through silicate liquid immiscibility from the literature (see Rajesh 1999 for the compilation of data). The latter studies show that the enrichment of Ti and P in the basic liquid (silica-depleted) over the felsic liquid (silica-rich) is proportional to the difference in the degree of polymerization of these liquids as approximated by the ratio of the silica contents. The behavior of Puttetti sample pairs in Fig. 9 is comparable to similar immiscible pairs from various studies

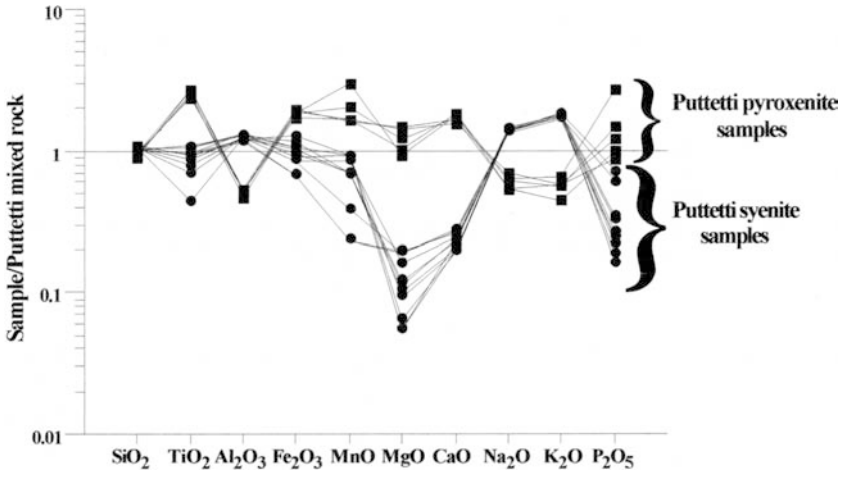

Fig. 7 Major element concentrations in Puttetti syenite and pyroxenite samples normalized to the corresponding concentrations in the mixed-rock

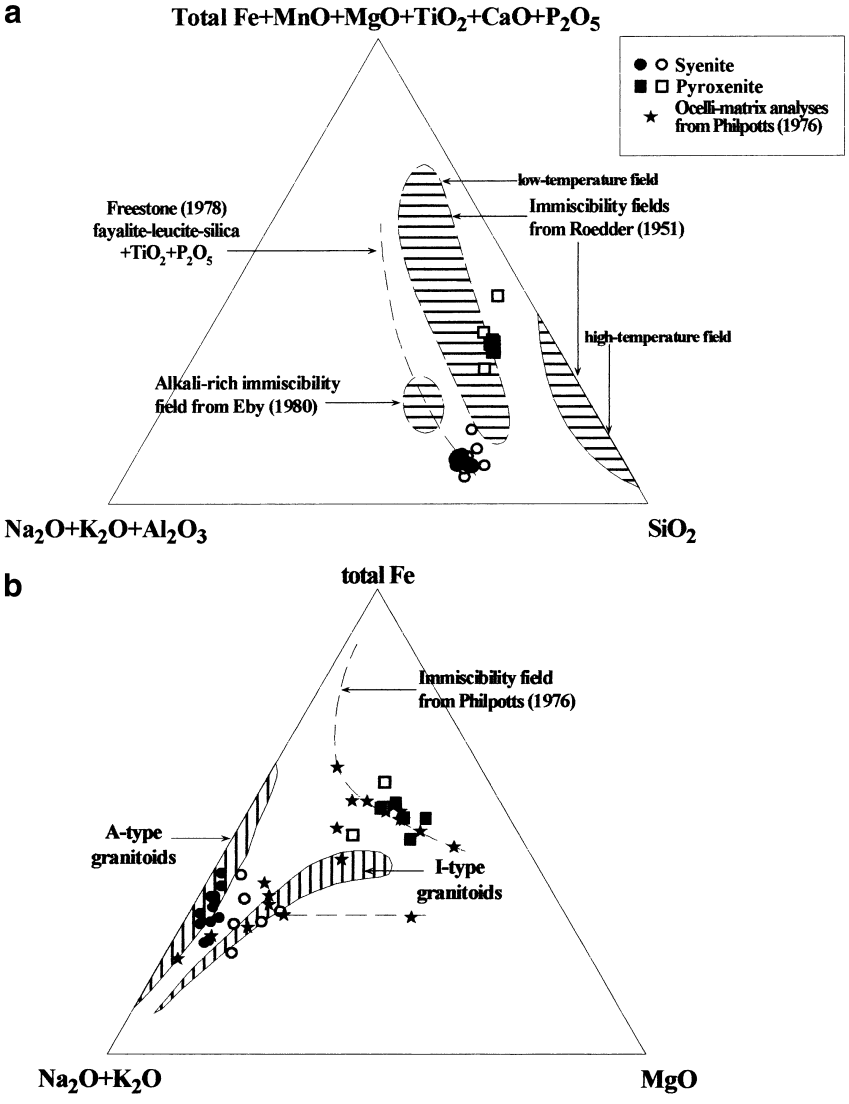

Fig. 8 **a** Pseudo-ternary diagram for the system leucite-fayalite-silica, from Roedder (1951), showing the two fields of potential liquid immiscibility (*large elliptical areas*) and the compositions of the Puttetti syenite, pyroxenite and mixed-rock. The *dashed line* is the immiscibility field produced by the addition of TiO_2 and P_2O_5 (Freestone 1978). The *small elliptical area* is the alkali-rich immiscibility field from Eby (1980). *Open symbols* are data from Nair and Santosh (1985) and *closed symbols* are from this study. **b** FMA (wt%) plot for the Puttetti syenite, pyroxenite and mixed-rock samples. The field of immiscibility for Monteregian dike rocks determined by Philpotts (1976) is shown by *dashed lines*. Ocelli-matrix analyses from Philpotts (1976) and general fields of A-type and I-type granitoids are also shown. *Open symbols* are data from Nair and Santosh (1985) and *closed symbols* are from this study

(e.g. ocelli-matrix pairs from Philpotts 1976, syenite-pyroxenite pairs from Ferreira et al. 1994) where the source rock is alkaline (e.g. see mixed-rock samples from this study and Ferreira et al. 1994 in Fig. 3), and slightly different from immiscible pairs (e.g. Fe-enriched basalt-plagiogranite pairs from Dixon and Rutherford 1979; glassy globules in basalts from Philpotts 1982) whose source rock is tholeiitic (e.g. see

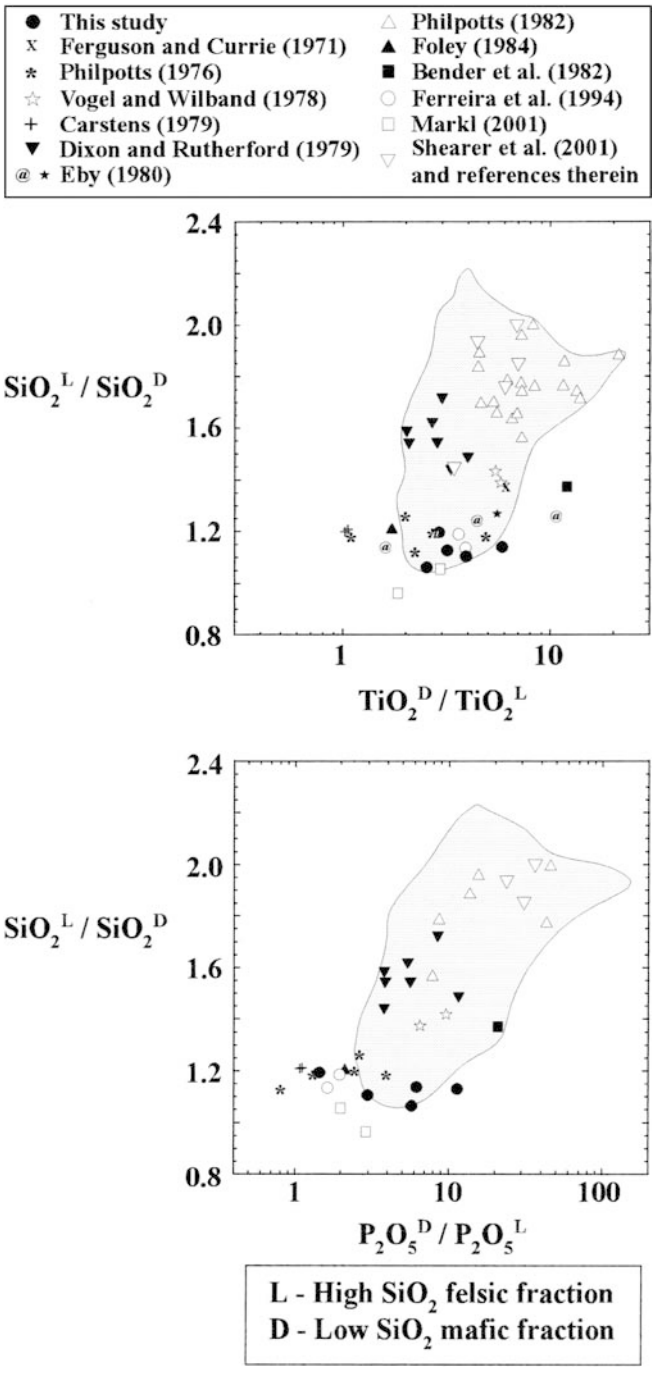

Fig. 9 Ratios of SiO_2, TiO_2 and P_2O_5 in representative syenite-pyroxenite pairs from Puttetti compared with those in natural and experimental glass pairs from literature (*shaded area*). Ocelli-matrix pair in alkaline ultrabasic rock from Ferguson and Currie (1971), ocelli-matrix pairs in the Monteregian alkaline province from Philpotts (1976), granite-basic rock pairs from Vogel and Wilband (1978), globule-matrix pairs in basic alkaline magmas from Carstens (1979), Fe-enriched basalt-plagiogranite pairs from Dixon and Rutherford (1979), syenite-nepheline diorite pair (*filled star*) and ocelli-matrix pairs (@) in lamprophyre from Eby (1980), glassy globules in tholeiitic basalts from Philpotts (1982), granodiorite-diorite pair from Bender et al. (1982), globule-matrix pair in alkaline lamprophyres from Foley (1984), syenite-pyroxenite pairs from Ferreira et al. (1994), unmixed melts in nepheline syenites from Markl (2001), and experimental and lunar immiscible melt pairs from Shearer et al. (2001) and references therein are also shown

basalts from Dixon and Rutherford 1979 and Philpotts 1982 in Fig. 3).

Like major elements, trace elements also show similar evolutionary trends between the three rock types (Fig. 10). Abundance of high charge density (HCD) cations such as Ga, Zr, Zn, Nb is prominent for syenite, owing to the incompatible nature of these elements in A-type magmas. Incompatible element partitioning between syenite and pyroxenite liquids (Fig. 11a) indicates that except for Rb, Zr, Nb in the syenite other elements show higher concentrations in the pyroxenite. Trace element patterns of the Puttetti rocks, with mixed rock patterns intermediate between those of pyroxenite and syenite, (Fig. 11a) are comparable with those of immiscible pairs from literature.

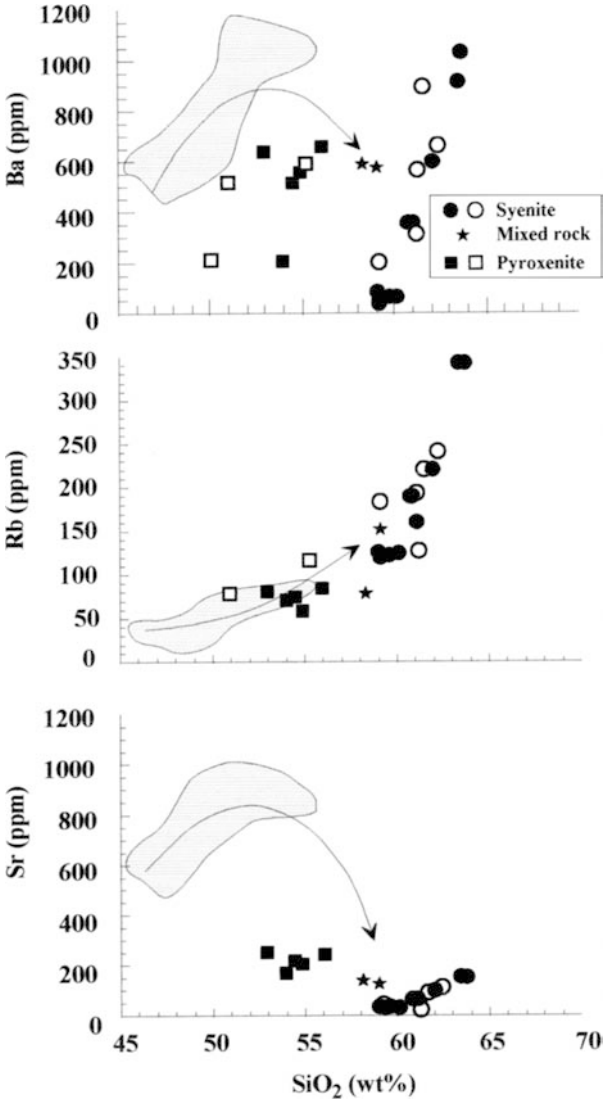

Fig. 10 Representative trace element variation diagrams of the Puttetti syenite, pyroxenite and mixed-rock samples. *Open symbols* are data from Nair and Santosh (1985) and *closed symbols* are from this study. Data from Gough Island basalts (*shaded area*) and the corresponding trends (*dotted line*) of crystal fractionation of these basaltic magmas to generate intermediate rocks is also shown

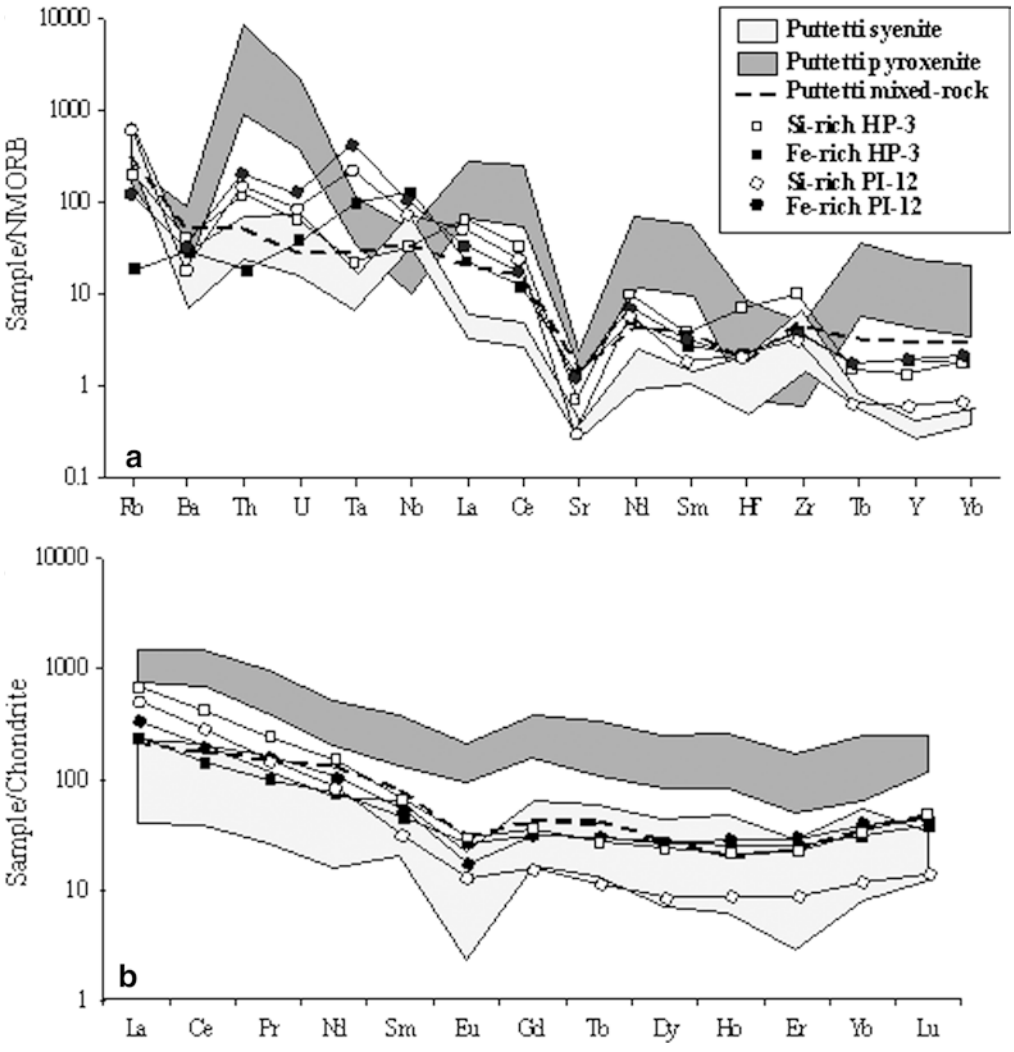

Fig. 11 a MORB normalized element patterns for the Puttetti syenite, pyroxenite and mixed-rock samples. Si-rich–Fe-rich immiscible pairs in syenitic xenoliths (sample nos. HP-3 and PI-12) from Hurai et al. (1998) is shown for comparison. **b** Chondrite-normalized REE patterns for the Puttetti syenite, pyroxenite and mixed-rock samples. Si-rich–Fe-rich immiscible pairs in syenitic xenoliths (sample nos. HP-3 and PI-12) from Hurai et al. (1998) is shown for comparison (see text for details)

Calculated NBO/T (non bridging oxygens/tetrahedrally coordinated cations) ratios for the Puttetti samples [$(NBO/T)_{syenite}/(NBO/T)_{pyroxenite} = 0.162–0.187$; Rajesh 1999; for calculation procedure see Eby 1980] and linear HCD cation partitioning patterns indicate that the HCD cations (except Zr, Nb) will be partitioned into the basic melt as is observed by the trends of the Puttetti syenite and pyroxenite (see Fig. 11a). The non-linear cation partitioning patterns of Zr and Nb may be due to the presence of solid phases, like zircon crystals, which may have been present when immiscibility occurred and could significantly distort the minor and trace element partitioning patterns (Eby 1980). In addition, minor amounts of CO_2, Cl or F may be effective in promoting immiscibility and HCD cations tend to concentrate in the volatile-enriched phase (Eby 1980). The presence of CO_2 is compatible with the Puttetti pluton with CO_2-rich fluid inclusions observed in zircon crystals from syenite (Santosh 1985; Rajesh 1999).

The REE patterns of the Puttetti syenite and pyroxenite are parallel with negative Eu anomalies, LREE enrichment and HREE depletion (Fig. 11b). Similarity of REE distribution between the mixed rock, having intermediate REE patterns between syenite and pyroxenite, and syenite and pyroxenite is compatible with unmixing. The REE abundance are higher in the pyroxenite than in the syenite (Fig. 11b) in accordance with the experimental work on immiscible liquids by Ellison and Hess (1989) which showed that REE are preferentially partitioned into the Fe-rich liquid. This is contrary to any model involving fractionation or partial melting, which, in either case, yields increasing enrichment in the quartzofeldspathic member. There are exceptions in the literature, like the Si-rich and Fe-rich immiscible pairs in syenitic xenoliths from the Pannonian Basin (Hurai et al. 1998), where REE (especially LREE) are partitioned into the Si-rich liquid (see Fig. 11b) and is attributed to the extraction of a high-iron-oxide melt from the system (see Hurai et al. 1998 for details). However, the fractionated REE patterns with more pronounced Eu anomalies and LREE/HREE ratios of the Puttetti syenite and pyroxenite in comparison with the mixed-rock needs to be explained. Feldspar crystallization can account for the more pronounced Sr and Eu anomaly in Puttetti syenite. The difference in Eu

behavior reflects the similarity of divalent Eu to Sr rather than to the other trivalent REE. Indeed, during liquid immiscibility, the REEs should behave in a coherent fashion and exhibit similar two-liquid partition coefficients (e.g. Watson 1976). But precipitation of an accessory phase, like zircon (in this case), accompanying silicate liquid immiscibility can produce a fractionated REE pattern (similar to this study) as has been documented for lunar immiscible melts (e.g. Snyder et al. 1993). Hence, the immiscible separation of the Puttetti mixed rock causes REE fractionation, resulting in the LREE enriched and HREE depleted immiscible fractions. It is also possible, that a late stage CO_2 vapor (?) could have affected the elemental distribution as evidenced by the widespread occurrence of calcite.

Conditions of crystallization

Temperature estimates based on zircon solubilities in felsic liquids (Watson and Harrison 1983) range from ~980 to ~900 °C for the Puttetti syenite. There is no evidence for inherited zircon as separates used by previous geochronological studies show euhedral prismatic zircon crystals of magmatic origin. Similar high temperatures were obtained when compared with the Fe-Ti oxide saturation isotherms of Green and Pearson (1986). Relatively high temperatures >900 °C—typical of water-deficient alkali granitoid—are indicated by simple zircon morphology (combinations of first-order pyramidal [101] and prismatic [100] forms; Pupin 1980). Comparison with experimental studies suggests the composition of the Puttetti syenite would be consistent with liquidus temperatures in the range of 900–1,000 °C (Tuttle and Bowen 1958; James and Hamilton 1969; Nekvasil and Lindsley 1990). Such high temperatures suggest a relatively early stage of differentiation of the parent magma.

Isotope systematics and tectonic scenario

U-Pb zircon ages of 580 ± 10 Ma (Odom 1982) and 572 ± 2 Ma (Kovach et al. 1998) have been reported for the syenite. Interestingly, this age is similar to the Rb-Sr age (572 Ma; initial $^{87}Sr/^{86}Sr$ ratio = 0.7098) reported for the ultrapotassic syenite-pyroxenite association from Triunfo pluton, northeastern Brazil considered to be an example for large-scale silicate liquid immiscibility (Ferreira et al. 1994). Radiogenic isotope ratios in associated syenite and pyroxenite rocks provide a necessary condition for an origin as immiscible liquid fractions: at the time of unmixing, immiscible fractions must have the same ratios of parent and daughter isotopes. Initial isotope ratios should be independent of crystal fractionation. Sr-isotopic analyses of Puttetti samples were performed on an MAT261 mass spectrometer equipped with five Faraday cups following the analytical procedure described by Kagami et al. (1987). The measured $^{87}Sr/^{86}Sr$ ratio of NBS987 during this study (0.710239) compared favourably with that reported for NBS987 by Kagami et al. (1987).

Rb/Sr analyses of Puttetti syenite and pyroxenite samples give initial Sr isotope ratios of 0.70717–0.70846 at 572 Ma (Table 3). Because the syenite and pyroxenite have similar strontium isotopic initial values, they could be related by a common process.

Eby (1992) suggested that the Y/Nb ratio could distinguish among A-type granitoids with mantle (Y/Nb < 1.2) or crustal (Y/Nb > 1.2) origins. Most of the Puttetti syenite samples have Y/Nb < 1.2, implying that they are largely mantle in origin. Further they belong to the A_1 sub group of Eby (1992), which includes anorogenic granitoids that are mantle derived and emplaced during extension or continental rifting. Conventional tectonic discrimination diagrams of Pearce (1996) indicate that the majority of the Puttetti syenite samples have within-plate characteristics with some samples straddling the boundary between the fields of WPG and VAG, similar to Pan-African post-collisional potassic granitoids from NE Africa (see Küster and Harms 1998), syenites from Madagascar (Nédélec et al. 1995), and syenites from Yamato mountains, East Antarctica (Zhao et al. 1995; Fig. 12). In a super continent framework, the 572 Ma Puttetti syenite belongs to the most intensive period of A-type granitoid activity (580–540 Ma; see Rajesh 2003) along the Gondwana suture [the continuation of the East African orogen (Stern 1994) into the East Antarctic orogen (Jacobs et al. 1998)] in a post-collisional extensional setting, the collision being that of fragments of East and West Gondwana.

Petrogenetic implications

It has now become clear that the generation of A-type granitoids involve multiple processes, including partial melting, fractional crystallization, metasomatism, liquid immiscibility, crustal contamination, halide complexing and thermo-gravitational diffusion (see Collins et al. 1982 and references therein). Previous studies on southwestern Indian A-type granitoids (e.g. Rajesh, 2000) have suggested that diversification of these A-type granitoid magmas would largely depend upon the source characteristics, extent of partial melting, and modifica-

Table 3 Rb-Sr isotopic data for the Puttetti syenite and pyroxenite

Sample	Rb (ppm)	Sr (ppm)	$^{87}Rb/^{86}Sr$	$^{87}Sr/^{86}Sr$	Sr I (572 Ma)
PU-1s[a]	26.89	160.91	0.48366	0.71111	0.70717
PU-2s	72.50	224.20	0.93628	0.71513	0.70750
PU-3s	91.03	203.99	1.29238	0.71774	0.70720
PU-4s	27.46	133.43	0.59571	0.71245	0.70759
PU-5s	137.30	406.91	0.97699	0.71541	0.70745
PU-1p[b]	18.52	146.64	0.36552	0.71094	0.70796
PU-2p	16.21	161.12	0.29116	0.71012	0.70775
PU-3p	21.24	169.31	0.36309	0.71142	0.70846

[a]Syenite
[b]Pyroxenite

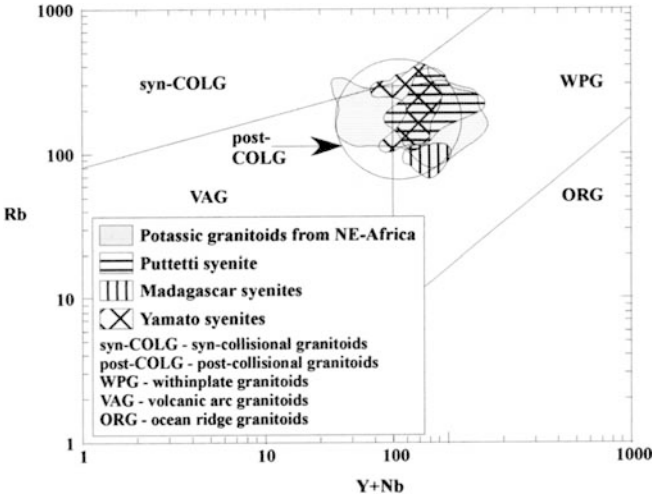

Fig. 12 Rb vs. Y + Nb tectonic discrimination diagram (Pearce 1996) for Puttetti syenite. Data from Pan-African post-collisional potassic granitoids from NE-Africa (average values compiled by Küster and Harms 1998), syenites from Madagascar (Nédélec et al. 1995) and syenites from Yamato mountains, East Antarctica (Zhao et al. 1995) are also shown

tion of the melt by fractional crystallization, with each taking lead at a particular stage of magma evolution. Silicate liquid immiscibility, although not often suggested for A-type granitoid petrogenesis, is a viable model for the origin of the Puttetti syenite (A-type granitoid) and associated pyroxenite.

Field evidence for the contemporaneous nature of syenitic and pyroxenitic liquids, the occurrence of the mixed-rock with an emulsion-like texture, and the occurrence of pyroxenite globules in syenite, may reasonably be interpreted as relics of immiscible magmas with the unmixing of the mixed-rock liquid initiated by the separation of rounded globules of the pyroxenitic phase in a syenitic matrix. Both syenite and pyroxenite show similar mineral assemblage (with major minerals having overlapping chemical compositions), but the relative proportions differ. Overlapping mineral compositions are consistent with petrogenesis by liquid immiscibility, i.e., identical compositions in rocks derived from felsic and mafic magmas, are extremely unlikely if the rocks are unrelated or are related by fractional crystallization, partial melting, assimilation, etc. Major element partitioning trends and the presence of a compositional gap in a pseudo-ternary Greig diagram are in accord with the silicate liquid immiscibility model of origin. In most cases, the partitioning behavior of the trace elements agrees with behavior either predicted or measured for immiscible melts in experimental and/or natural systems. Immiscibility can also account for the REE distribution difference between the syenite and pyroxenite, with the more pronounced Eu anomalies and LREE/HREE ratios of syenite and pyroxenite (relative to the mixed-rock) related to fractionation caused by immiscible separation. Further both syenite and pyroxenite have similar Sr isotopic compositions. Thus the proposed origin of the Puttetti pluton involves the intrusion of a mixed-rock magma whose bulk composition is that of approximately 70% syenitic and 30% pyroxenitic units. This melt behaved immiscibly and split into two fractions, which produced the syenite and pyroxenite rocks.

Comparison with recent experimental studies allows reasonable approximations regarding the nature of the possible source for the Puttetti mixed-rock. In the various discriminant diagrams available for volcanic rocks, the mixed-rock samples fall in the basaltic field (e.g. Fig. 13) and along the trend of crystal fractionation from alkali basalt (e.g. Figs. 3, 13). Models involving fractional crystallization from basaltic parent magma require that depletion of compatible elements must occur along with enrichment in incompatible elements. Fractionation of basalt to intermediate compositions

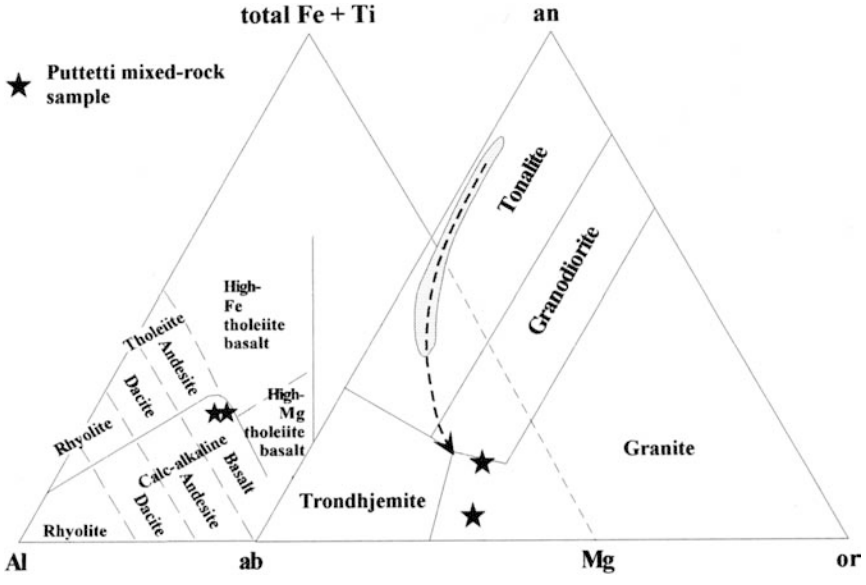

Fig. 13 Mixed-rock compositions in a cation percentage triplot of Al, (total Fe + Ti) and Mg showing the classification of volcanic rocks, and in a normative an–ab-or ternary diagram. Data from Gough Island basalts (*shaded area*) and the corresponding trends (*dotted line*) of crystal fractionation of these basaltic magmas to generate intermediate rocks is also shown

would involve removal of plagioclase, producing a negative Eu anomaly and depletion of Sr, which has occurred in the Puttetti mixed-rock. Likewise, generally good major and trace element matches are found between the fractionation trends of basalt (e.g. Gough island basalts; Le Roex 1985) and Puttetti mixed rock, lending support to a fractionation model (e.g. see Figs. 6, 10, 13). Thus a period of basaltic under plating is favored, with the ponding of mafic magmas, the fractionation of which results in the formation of the Puttetti mixed-rock.

As far as the extent of this silicate liquid immiscbility is concerned, Ferreira et al. (1994) pointed out that the large scale silicate liquid immiscibility they reported between the ultrapotassic syenite and pyroxenite in the Triunfo batholith (the largest of the plutons in the Cachoeirinha-Salgueiro fold belt (CSF) northeastern Brazil) may be a major magmatic process in the generation of other ultrapotassic syenite plutons in the CSF. In South India, this study accounts for silicate liquid immiscibility between syenite and pyroxenite at an outcrop scale near Puttetti, less extensive than in the case of Triunfo batholith. A number of alkaline plutons (e.g. Yelagiri, Sevattur plutons) comprising syenite, pyroxenite and carbonatite have been reported from the northeastern part of the South Indian shield and are located along a major NE–SW tending lineament (Grady 1971). Miyazaki et al. (2000) reported similar Sr initial isotope characteristics for syenite and pyroxenite of the Sevattur pluton at 756 Ma. They also reported a whole-rock Rb-Sr isochron age of 757 Ma for the Yelagiri syenite too, but no isotope study was done on the pyroxenite body. Although field relations are not clear and detailed geochemical studies needs to be done on these plutons, silicate liquid immiscibility seems an interesting petrogenetic option to be tested. Silicate liquid immiscibility may have been much more common than previously supposed during late Precambrian times.

Acknowledgements Kagami, Miyazaki and Ali are thanked for their assistance in Rb-Sr analysis and discussions. Osanai, Ueno, Suzuki and Doyama are acknowledged for their hospitality, and analytical facilities. Akai, Ueno and Okudaira are thanked for their analytical assistance at various stages. Comments by Watson and Naslund helped in making the manuscript concise and focused. Editorial suggestions by Grove were valuable. This is a contribution to the MONBUSHO Grant-in-Aid for Scientific Research (A) No. 13373005, and IGCP 453.

References

Balaram V, Ramesh SL, Anjiah KV (1996) New trace element and REE data in thirteen GSF reference samples by ICP-MS. Geostandards Newsl 20:71–78

Bence AE, Albee AL (1968) Empirical correlation factors for the electron microanalysis of silicates and oxides. J Geol 76:382–402

Bender JF, Hanson GN, Bence AE (1982) The Cortlandt complex: evidence for large-scale liquid immiscibility involving granodiorite and diorite magmas. Earth Planet Sci Lett 58:330–344

Bowen NL (1928) The evolution of the igneous rocks. Princeton University Press, Princeton, 332 pp

Carstens H (1979) Liquid immiscibility in basic alkaline magmas. Chem Geol 27:297–307

Collins WJ, Beams SD, White AJR, Chappell BW (1982) Nature and origin of A-type granites with particular reference to southeastern Australia. Contrib Mineral Petrol 80:189–200

Cox KG, Bell JD, Pankhurst RJ (1979) The interpretation of igneous rocks. George Allen and Unwin, London, 450 pp

Dixon S, Rutherford MJ (1979) Plagiogranites as late-stage immiscible liquids in ophiolite and mid-ocean ridge suites: an experimental study. Earth Planet Sci Lett 45:45–60

Eby GN (1980) Minor and trace element partitioning between immiscible ocelli-matrix pairs from lamprophyre dykes and sills, Monteregian hills petrographic province, Quebec. Contrib Mineral Petrol 75:269–278

Eby GN (1992) Chemical subdivision of A-type granitoids: petrogenesis and tectonic implications. Geology 20:641–644

Ellison AJG, Hess PC (1989) Solution properties of rare earth elements in silicate melts: inferences from immiscible liquids. Geochim Cosmochim Acta 53:1965–1974

Ferguson J, Currie KL (1971) Evidence of liquid immiscibility in alkaline ultrabasic rocks at Celendar bay, Ontario. J Petrol 12:561–585

Ferreira VP, Sial AN, Whitney JA (1994) Large-scale silicate liquid immiscibility: a possible example from northeastern Brazil. Lithos 33:285–302

Foley, SF (1984) Liquid immiscibility and melt segregation in alkaline lamprophyres from Labrador. Lithos 17:127–137

Freestone IL (1978) Liquid immiscibility in alkali-rich magmas. Chem Geol 23:115–123

Frost BR, Barnes CG, Collins WJ, Arculus RJ, Ellis DJ, Frost CD (2001) A geochemical classification for granitic rocks. J Petrol 42:2033–2048

Grady JC (1971) Deep main faults in South India. J Geol Soc India 12:56–62

Green TH, Pearson NJ (1986) Ti-rich accessory phase saturation in hydrous mafic-felsic compositions at high P, T. Chem Geol 54:185–201

Halsor SP, Rose WI (1991) Mineralogical relations and magma mixing in calc-alkaline andesites from Lake Atitlan, Guatemala. Mineral Petrol 45:47–67

Hibbard MJ (1981) The magma mixing origin of mantled feldspars. Contrib Mineral Petrol 76:158–170

Hurai V, Simon K, Wiechert U, Hoefs J, Konečný P, Huraiova M, Pironon J, Lipka J (1998) Immiscible separation of metalliferous Fe/Ti-oxide melts from fractionating alkali basalt: P–T–fO_2 conditions and two-liquid elemental partitioning. Contrib Mineral Petrol 133:12–29

Jacobs J, Fanning CM, Henjes-Kunst F, Olesch M, Paech H-J (1998) Continuation of the Mozambique belt into East Antarctica: Grenville-age metamorphism and polyphase Pan-African high-grade events in central Dronning Maud Land. J Geol 106:385–406

James RS, Hamilton DL (1969) Phase relations in the system $NaAlSi_3O_8$–$KAlSi_3O_8$–$CaAl_2Si_2O_8$ at 1 kb vapor pressure. Contrib Mineral Petrol 21:111–141

Kagami H, Iwata M, Sano S, Honma H (1987) Sr and Nd isotopic compositions and Rb, Sr, Sm and Nd concentrations of standard samples. Tech Rep ISEI, Okayama Univ Ser B4:165–177

Kovach VP, Santosh M, Salnikova EB, Berezhnaya NG, Bindu RS, Yoshida M, Kotov AB (1998) U-Pb zircon age of the Puttetti alkali syenite, southern India. Gond Res 1:408–410

Kuscu GG, Floyd PA (2001) Mineral compositional and textural evidence for magma mingling in the Saraykent volcanics. Lithos 56:207–230

Küster D, Harms U (1998) Post-collisional potassic granitoids from the southern and northwestern parts of the late Neoproterozoic East African Orogen: a review. Lithos 45:177–195

Le Roex AP (1985) Geochemistry, mineralogy and magmatic evolution of the basaltic and trachytic lavas from Gough island, South Atlantic. J Petrol 26:149–186

Markl G (2001) A new type of silicate liquid immiscibility in peralkaline nepheline syenites (lujavrites) of the Ilimaussaq complex, South Greenland. Contrib Mineral Petrol 141:458–472

Miyazaki T, Kagami H, Shuto K, Morikyo T, Mohan VR, Rajasekaran KC (2000) Rb-Sr geochronology, Nd-Sr isotopes and whole rock geochemistry of Yelagiri and Sevattur syenites, Tamil Nadu, South India. Gond Res 3:39–53

Murali AV, Parthasarathy R, Mahadevan TM, Sankardas M (1983) Trace element characters, REE patterns and partition coefficients of zircons from different geological environments – a case study of Indian zircons. Geochim Cosmochim Acta 47:2047–2052

Nair NGK, Santosh M (1985) Geochemistry and petrogenesis of the Puttetti syenite, South India. Neues Jahrb Miner Abh 151:213–227

Nandakumar V, Harley SL (2000) A reappraisal of the pressure-temperature path of granulites from the Kerala Khondalite Belt, southern India. J Geol 108:687–703

Naslund HR (1983) The effect of oxygen fugacity on liquid immiscibility in iron-bearing silicate systems. Am J Sci 283:1043–1059

Nédélec A, Stephens WE, Fallick AE (1995) The Pan-African stratoid granites of Madagascar: alkaline magmatism in a post-collisional extensional setting. J Petrol 36:1367–1391

Nekvasil H, Lindsley DH (1990) Determination of the 2 feldspar + liquid curve in the system An–Or–An–H_2O at low H2O contents. Am Mineral 75:1071–1079

Odom AL (1982) Isotope age determinations of rock and mineral samples from Kerala, India. Final Rep UN Case No 81-10084, 10 pp

Pearce JA (1996) Sources and settings of granitic rocks. Episodes 19:120–125

Philpotts AR (1976) Silicate liquid immiscibility: its probable extent and petrogenetic significance. Am J Sci 276:1147–1177

Philpotts AR (1978) Textural evidence for liquid immiscibility in tholeiites. Mineral Mag 42:417–425

Philpotts AR (1982) Compositions of immiscible liquids in volcanic rocks. Contrib Mineral Petrol 80:201–218

Pupin JP (1980) Zircon and granite petrology. Contrib Mineral Petrol 73:207–220

Rajesh HM (1999) Characterization and origin of alkaline and calc-alkaline aluminous A-type granitoids from southwestern India: implications for Gondwanaland tectonics. DSc Thesis Osaka City University, Japan, 317 pp

Rajesh HM (2000) Characterization and origin of a compositionally zoned aluminous A-type granite from South India. Geol Mag 137:291–318

Rajesh HM (2003) The igneous charnockite—A-type granite—arrested charnockite association in southwestern India: implications for the Pan-African Post-collisional extensional collapse along the Gondwana suture. (submitted)

Rajesh HM, Santosh M, Yoshida M (1996) The felsic magmatic province in East Gondwana: implications for Pan-African tectonics. J Southeast Asian Earth Sci 14:275–291

Roedder E (1951) Low-temperature liquid immiscibility in the system K_2O-FeO-Al_2O_3-SiO_2. Am Mineral 36:282–286

Roedder E (1979) Silicate liquid immiscibility in magmas. In: Yoder HS Jr (ed) The evolution of the igneous rocks. 50th Anniversary Perspective. Princeton University Press, Princeton, pp 15–57

Santosh M (1985) Crystal growth of zircons in Puttetti syenite as recorded from fluid inclusions. J Geol Soc India 26:695–703

Satishkumar M, Harley SL (1998) Reaction textures in scapolite-wollastonite-grossular calc-silicate rock from the Kerala Khondalite Belt, southern India: evidence for high-temperature metamorphism and initial cooling. Lithos 44:83–99

Shearer CK, Papike JJ, Spilde MN (2001) Trace-element partitioning between immiscible lunar melts: an example from naturally occurring lunar melt inclusions. Am Mineral 86:238–246

Snyder GA, Taylor LA, Crozaz G (1993) Rare earth element selenochemistry of immiscible liquids and zircon at Apollo 14: an ion probe study of evolved rocks on the Moon. Geochim Cosmochim Acta 57:1143–1149

Stern RJ (1994) Arc assembly and continental collision in the Neoproterozoic East African orogen: implications for the consolidation of Gondwanaland. Ann Rev Earth Planet Sci 22:319–351

Tuttle OF, Bowen NL (1958) Origin of granite in the light of experimental studies in the system $NaAlSi_3O_8$–$KAlSi_3O_8$–SiO_2–H_2O. Geol Soc Am Mem 74:153 pp

Vernon RH (1983) Restite, xenoliths and microgranitoid enclaves in granites. J Proc R Soc NSW 116:77–103

Vogel TA, Wilband JT (1978) Coexisting acidic and basic melts: geochemistry of a composite dike. J Geol 86:353–371

Watson EB (1976) Two-liquid partition coefficients: Experimental data and geochemical applications. Contrib Mineral Petrol 56:19–34

Watson EB, Harrison TM (1983) Zircon saturation revisited: temperature and composition effects in a variety of crustal magma types. Earth Planet Sci Lett 64:295–304

Wiebe RA (1993) The Pleasant Bay layered gabbro-diorite, Coastal Mine: ponding and crystallization of basaltic injections into a silicic magma chamber. J Petrol 34:461–489

Zhao J-X, Shiraishi K, Ellis DJ, Sheraton, JW (1995) Geochemical and isotopic studies of syenites from the Yamato mountains, East Antarctica: implications for the origin of syenitic magmas. Geochim Cosmochim Acta 59:1363–1382